LA-UR- 98 187

LA-UR--98-187

Approved for public release; distribution is unlimited.

Title: STRUCTURAL EFFECTS IN ICF FOAM-BUFFERED TARGETS

CONF-971082--

Author(s): Rodney J. Mason, X-PA
Roger A. Kopp, X-PA
S. Robert Goldman, X-PA
Douglas, C. Wilson, X-TA
Robert G. Watt, P-24

RECEIVED
MAY 28 1998
OSTI

Submitted to: For inclusion in the Proceedings of the 11th Biennial Nuclear Explosives Design Physics Conference,'97 NEDPC, Livermore, CA, Oct. 20-24, 1997.

Los Alamos
NATIONAL LABORATORY

Structural effects in ICF foam-buffered targets (U)

R. J. Mason, R. A. Kopp, S. R. Goldman, D. C. Wilson, and R. G. Watt
Los Alamos National Laboratory, Los Alamos, NM 87545

Experiments have indicated that low-density foam buffer layers can significantly mitigate the perturbing effects of beam non-uniformities in direct drive laser-matter interactions. A smooth drive is essential to obtaining ignition in the Direct Drive approach to ICF ignition. Consequently, we have conducted a detailed study of the mitigating capabilities of foam-buffers, and how to optimize them. Smoothly driven implosions may prove crucial to obtaining the high energy and neutron yields needed for Science Based Stockpile Stewardship applications.(U)

Introduction

In recent experiments to investigate the beam smoothing benefits of foam buffering *Dunne et al. (1996)* used targets consisted of 50 μm of 50 mg/cm^3 $C_{10}H_8O_4$ foam attached to a 10 μm foil and covered with 250 Å of gold, as shown in Fig. 1 (a). These targets have been exposed to ~1.2 ns, flat topped, green light (λ = 0.53 μm) pulses at ~1.4 x 10^{14} W/cm^2 intensity [Fig. 1 (b)], bearing 10 to 60 μm lateral perturbations. Without the buffer layers the foils were severely disrupted after 1 ns of laser illumination. Buffering can provide stability for more than 2 ns of full shell acceleration.

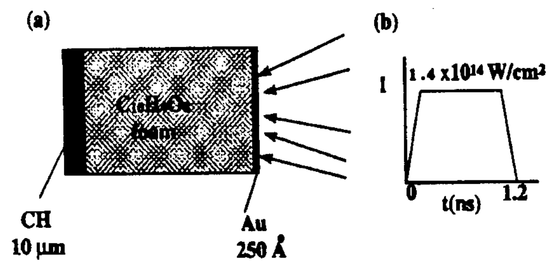

Figure 1. a) Typical foam-buffered target. Light strikes a gold over-layer from the right. b) Flat-topped pulse used for experiments on the LANL TRIDENT glass laser system.

It is instructive to see how the individual elements contribute to the dynamics of the foam buffer package.

Calculational Results

First consider radiation from a gold layer separated some distance from the foam. For the LASNEX results of Fig. 2 (a) we used 1500 Å of gold, *detached* and displaced 3000 μm to the right of the foam. The laser arrived from the right. No CH layer was present at the left of the foam. The foam was 200 μm long. The gold was irradiated with 0.5 μm light, and at a peak intensity of 1.4 x 10^{14} W/cm^2, delivered with the 1.2 ns, Fig. 1 (b) flat pulse. We see that an electron temperature T_e front penetrates the foam, such that the 80 eV frontal point moves at 2.1 x 10^7 cm/s. The radiation first strikes the foam at the right, and raises the electron temperature there. The subsequent penetration is supersonic, in that the density increase behind is only ~10%. The electron temperature increases are due to radiative penetration. This follows from observations that when either a tiny electron flux limiter, e.g. f_e = 10^{-3}, or a miniscule electron thermal conductivity multiplier is employed, e.g. K_{em} = 10^{-4}, the T_e penetration rate is only negligibly altered. LASNEX also tells us that the mean radiation temperature T_r (over the 73 groups used in our calculation) is only slightly above the electron temperature at the driver side of the foam. At 200 ps, for example, T_r(z = 200 μm) = 110 eV with T_e(200) = 100 eV. However, much deeper into the foam and at 800 ps the radiation front clearly leads the electron temperature profile –

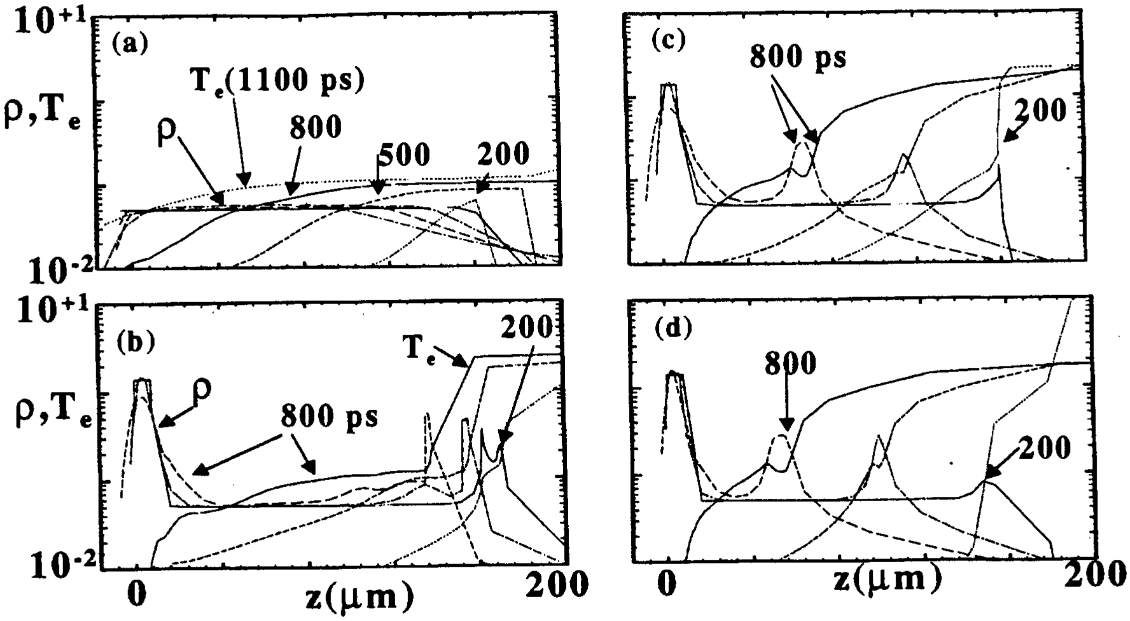

Figure 2. Evolving electron temperature T_e (keV) and plasma density ρ (gm/cm^3) under the Fig. 1 (b) pulse for: a) a 1500 Å gold layer displaced 3000 Å to the right of the foam, (b) the same gold layer directly attached to the foam and with a CH layer added behind the foam, (c) with the gold layer reduced to just 250 Å, and (d) with the gold layer replaced by 1 μm of CH. Progressively, stronger shocks are seen as the gold layer is first attached and then thinned.

with $T_r(z = 0) = 60$ eV, while $T_e(0) = 10$ eV. We are observing an "ionization wave", since as T_e rises above 70 eV, we find that the average level of ionization Z_{eff} rises above 2.5 -- from its initial code default value of 10%. These results are in accord with the supersonic ionization fronts seen by *Afshar-rad et al.* (1994). They used, however, a higher intensity, 10^{15} W/cm^2 in a 1.3 ns Full-width half-maximum Gaussian pulse, which produced faster, 3.5 x 10^7 cm/s penetration, but a similar weak subsequent 10% density pulse.

The scenario changes significantly when the gold has been deposited directly on the foam. For the Fig. 2 (b) LASNEX results we moved the 1500 Å gold layer up to the foam surface, and added a 10 μm CH foil at its opposite end. In this case, we see that the gold layer expands and yet survives until 800 ps, driving a shock with a two-fold density increase ahead of itself. More notably, the ionization front at 800 ps runs strongly ahead of the shock and continues to resemble the corresponding front of Fig. 2 (a). So with the thick gold layer attached, we have a weak shock preceded by strong ionization wave. Next, we reduced the gold thickness to 250 Å, as used in most of the experiments. Figure 2 (c) shows that by 500 ps (the middle set of curves in the frame) the foam density has been shocked four-fold, and the 80 eV T_e point is only slightly ahead of the density pulse. By 800 ps the electron temperature T_e is dropping rapidly through an ablation front in the foam. It is also shocked significantly to 130 eV on the leading edge of the density pulse, and spreads ahead as an ionization front (above 70 eV) for some 40 μm ahead of the pulse. Finally, Fig. 2 (d) collects results for no gold overcoat. We have replaced the gold outer layer with 1 μm of CH. (Essentially the same results are observed with 50 Å of gold.) At 500 ps the driven pulse is steeper, both on its shocked front, and at its ablating trailing edge. The electron temperature again drops rapidly through the ablation front, and drops much more rapidly ahead of the pulse than in the gold layered case. By 800 ps, and after 120 μm of foam has been crossed by the density pulse, the T_e front is again leaking

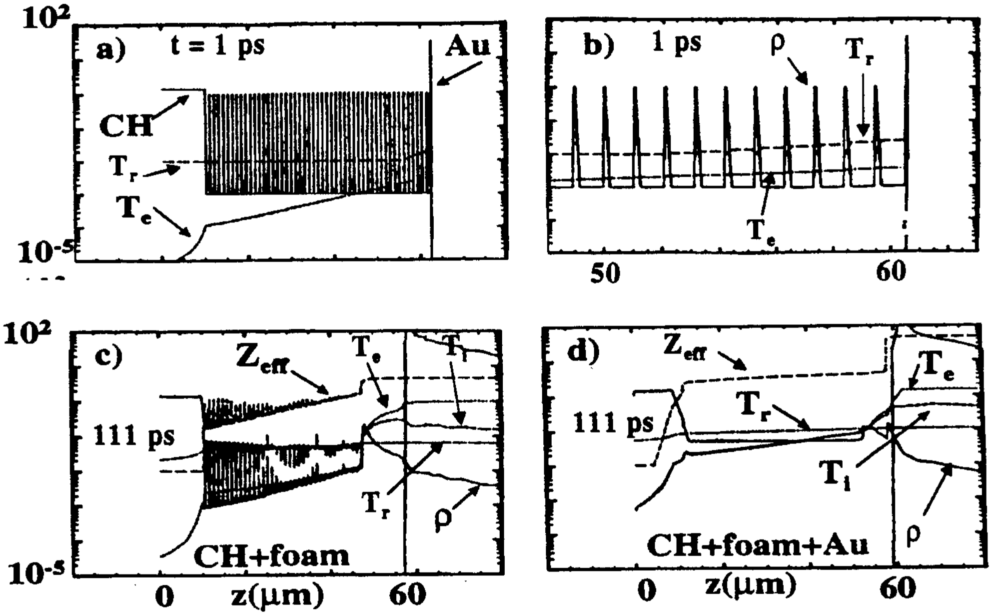

Figure 3. Evolution of a 50 mg/cm^3 structured foam system with 1 μm voids and intervening solid CH layers: a) density ρ (in g/cm^3), electron T_e and radiation T_r temperatures (in keV) at 1 ps, b) concomitant enlargement of the outermost foam and gold layers (between 48 and 60 μm), c) ragged conditions at 111 ps for CH and foam only (Z_{eff} is the degree of ionization), and d) corresponding nearly uniform foam conditions at the same time with CH plus foam and an added gold overlayer.

ahead, but less markedly than when the gold layer was present. In general, the separated thick gold layer produces a "pure" ionization wave followed by a 10% density pulse. Attachment of this 1500 Å of gold to the foam yields the same ionization wave and a trailing 60% density pulse. Thinning the gold to the 250 Å used in most experiments, gives a much stronger shock, i.e. a ~ 4/1 density pulse with the ionization front only slightly ahead of it -- during the crossing of the first 100 μm of foam. Finally, the use of less than 40 Å of gold restricts nearly all the ionization to the shock front, with little leakage ahead during the first 500 ps of the pulse.

Using LASNEX we have examined the effects of foam structure on the perturbation mitigation process. The foams used in experiments have voids spanning 1 to 3 μm. A gold outer layer on the foams greatly improves the smoothing of perturbations experimentally, although in simulation with uniform plasma foams little benefit from the gold is evident. Consequently, we have been studied possible smoothing limitations from the foam structure itself, and how a gold layer might alleviate such limitations. In one dimension we have carried out "picket fence" calculations as shown in Fig. 3. That is, we used spatial modulation of the foam density to mock up foam cells. In the upper left frame a) we see the initial plasma with 50 voids and 50 CH layers. Frame (b) is a blowup of the outermost foam and gold layers (between 48 and 60 μm). We have marked the density ρ, electron T_e and radiation T_r temperatures at 1 ps. Frame c) shows ragged conditions at 111 ps for CH and foam only (Z_{eff} is the degree of ionization), and d) displays corresponding nearly uniform foam conditions at the same time with CH plus foam and an added gold overlayer. The gold layer hastens conversion to a uniform-density plasma. Essentially, similar results were obtained when the void size was varied by up to a factor of 4.

For lower density, 10 mg/cm^3 foams the effects of structure in 1D are more obvious. For 3ω light, as used in foam experiments at Limeil and Rochester, the critical electron density is 9 x 10^{21} cm^{-3}. Our simulations show that by itself (in the absence of a gold layer) a uniform 10 mg/cm^3 foam never presents a critical surface to the incoming laser. On the other hand, when the foam

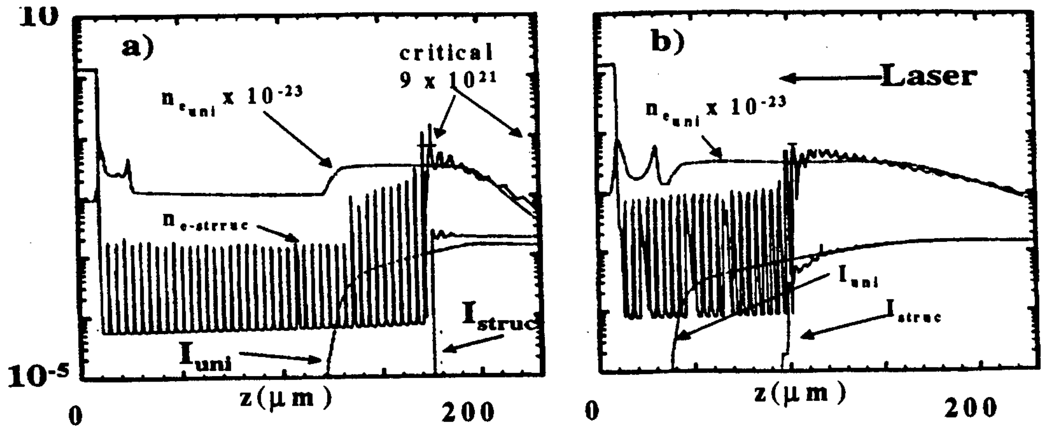

Figure 4. Comparison of the penetration of 0.35 μm light into structured and uniform 10 mg/cm^3 foams at: a) 100 ps and b) 200 ps under the Fig. 1 (b) pulse. The electron number density is in cm^{-3}, and the intensity in relative units. No critical surface is presented to the light (intensity I_{uni}) in the uniform case. The light (intensity I_{struc}) burns through a series of critical surfaces in the structured case.

is represented as a structured entity, the light stops at each critical surface progressively developed, as each solid layer is heated, ionized and collected by the shocked material driven by the laser. This contrast is evident in Fig. 4. It compares uniform and structured results for 200 μm of 10 mg/cm^3 foam exposed to our usual 1.4 x 10^{14} W/cm^2 pulse, but at 3ω. The structured foam was modeled with 50 voids, each of 4 μm width, and with thin intervening solid CH sheets. Frame (a) is for 100 ps and (b) is for 200 ps. In each case, we display the electron density profiles achieved, and the degree of penetration by the laser intensity I. At 100 ps this allows I to penetrate about 80 μm of the uniform foam, raising the electron density to a plateau value of 3.5 x 10^{21} e$^-$/cm^3, i.e. 0.4 n_{crit}. Absorption is by inverse-bremsstrahlung along this plateau. Alternatively, in the structured foam at 100 ps the light penetrates only 25 μm below the original foam surface, stopping at a critical surface presented by one of the CH sheets. Frame (b) shows that by 200 ps a front of subcritical density penetrates to 160 μm in the plasma that is initially uniform. Conversely, with the structure the light penetrates ~1.5 times more slowly - that is to 100 μm by 200 ps.

This is consistent with earlier findings (Tanaka et al, 1985) and an observed slowing of the shock penetration of foams in recent TRIDENT experiments, possibly bringing the transport rate for shocks in the foam into accord with recent experiments at AWE (Hoarty,1997).

From comparison of a series of runs for bare and buffered foils of various densities, we have found that foam-buffering can reduce both the amplitude and growth rate of imposed laser perturbations. Figure 5 collects the time dependent lateral mass shift $m_l = (\int\rho(t)dz - \int\rho(t=0)dz)/|\int\rho(t=0)dz|_{max\text{-}radially}$ for our usual 1.4 x 10^{14} W/cm^2 flat-topped pulse, with imposed 30 μm disturbances. Frame (a) for 60% level perturbations shows that with 50 μm of 50 mg/cm^3 foam the "ρz" shift starts later, and achieves only ~20% of the growth seen without foam. The semi-logarithmic plotting shows us that both the rate of growth and the peak amplitude are lower with the foam. Frame (b) for 100μm of foam and a weaker disturbance amplitude of δ = 0.1, shows that the growth is progressively slower, leading correspondingly to lower peak m_l values, in a sequence of runs in which the density of the foam is reduced.

Lower density foam may provide better smoothing, but earlier we indicated that at 10 mg/cm^3 an initially uniform gas foam model presented no critical surface to 3ω light. In 2D the result at 200 ps, following the Fig. 3 conditions, we find that there is an extreme distortion of the density in the foam and rapid breakup of the CH shell. However, the Fig. 3 study showed that initial foam structure can delay penetration into low density foams, possibly restoring their smoothing ability, and present a series of critical surfaces despite having and average density <n> less than n_{crit}.

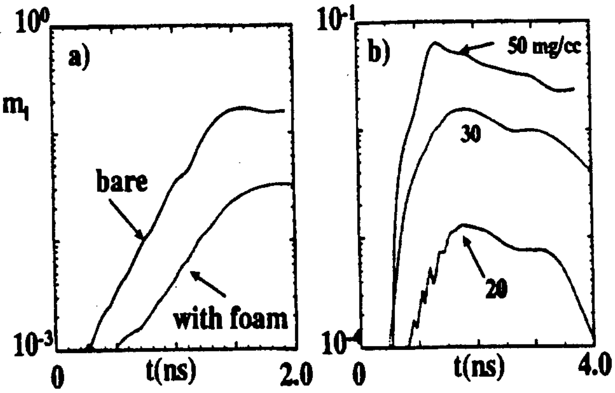

Figure 5. Relative instability growth for: a) bare and buffered 50 mg/cm^3 CH targets with a 60%, 30 μm wavelength perturbation, and for b) for 50, 30 and 20 mg/cm^3 foam buffers under 10% perturbed, 2ω laser illumination. Here m_l (see text) measures the lateral shift in mass.

Conclusion

Our simulations are the first to show comprehensively that: 1) a high level of electron thermal conduction is needed for the smoothing to be effective, 2) foam conversion to a uniform plasma, i.e. one without the initial void structure, substantially increases the electron conductivity, and 3) conversion aids smoothing in 2D. 4) The addition of a foam buffer layer limits both the growth rate and maximal amplitude of laser driven instabilities

References

Afshar-rad, T., Desselberger, M.., Dunne, M., Edwards, J., Foster, J.M., Hoarty, D., Jones, M. J., Rose, S. J., Roden, P. A., Taylor, R., and Willi, O., Phys. Rev. Lett. **73**, 74 (1994).

Dunne, M., Borghesi, M., Iwase, A., Jones, M., Taylor, M.. R., Willi, O., Gibson, Goldman, S. R., Mack, J., and Watt, R. G., *Phys. Rev. Lett.* **75**,3858 (1996).

Hoarty, D., AWE, private communication, May 1997.

Tanaka, K. A., Boswell, B., Craxton, R. S., Goldman, L. M., Guglielmi, F., Seka, W., Short, R. W., and Soures, M., Phys. Fluids **28**, 2910 (1985).

Watt, R. G., Wilson, D. C., Chrien, R. E., Hollis, R. V., Gobby, P. L., Mason, R. J., Kopp, R. A., Lerche, R. A., Kalantar, D. H., MacGowan, B., Nelson, M., B., Phillips, McKenty, P. W., and Willi, O., *Phys. Plasmas*, **4** 1379 (1997).

Report Number (14) LA-UR-- 98-187
CONF-971082--

Publ. Date (11) 199710
Sponsor Code (18) DOE/DP, XF
JC Category (19) UC-712, DOE/ER

DOE